

Controllable generation of highly nonclassical states from nearly pure squeezed vacua

Kentaro Wakui,^{1,2,3,*} Hiroki Takahashi,^{1,2,3} Akira Furusawa,^{2,3} and Masahide Sasaki^{1,3,†}

¹ *National Institute of Information and Communications Technology,
4-2-1 Nukui-Kita, Koganei, Tokyo 184-8795, Japan*

² *Department of Applied Physics, The University of Tokyo 7-3-1 Hongo, Bunkyo-ku, Tokyo 113-8656, Japan*

³ *CREST, Japan Science and Technology Agency, 1-9-9 Yaesu, Chuoh, Tokyo 103-0028, Japan*

We present controllable generation of various kinds of highly nonclassical states of light, including the single photon state and superposition states of mesoscopically distinct components. The high nonclassicality of the generated states is measured by the negativity of the Wigner function, which is largest ever observed to our knowledge. Our scheme is based on photon subtraction from a nearly pure squeezed vacuum, generated from an optical parametric oscillator with a periodically-poled KTiOPO₄ crystal as a nonlinear medium. This is an important step to realize basic elements of universal quantum gates, and to serve as a highly nonclassical input probe for spectroscopy and the study of quantum memory.

PACS numbers: 42.50.Dv, 03.65.Wj, 03.67.Mn

I. INTRODUCTION

Controllable generation of various kinds of nonclassical states of light is crucial for the study of fundamental aspects of quantum mechanics and developing quantum information science. One of effective methods is a conditional preparation scheme by photon counting on one part of an entangled state produced in the parametric down-conversion (PDC) [1, 2]. The main feature of the quantum states thus prepared is that their Wigner functions $W(x, p)$, which is a quasi-probability distribution for non-commuting quadrature observables $\hat{x}\hat{p} - \hat{p}\hat{x} = i$, should exhibit the negative values in certain phase-space regions. This is in sharp contrast to that a squeezed state, which are another representative of nonclassical states, have a non-negative definite Gaussian distribution of the Wigner function.

Generation and observation of nonclassical states with negative values of $W(x, p)$ have been reported recently. Those states can be categorized into two families. One family is the number states and their variants combined with coherent state components [3, 4, 5], created in a non-colinear PDC configuration of the signal and idler photons. The other is the photon subtracted squeezed states, where a small fraction of a squeezed vacuum beam is beam-split and guided into a photon counter as trigger photons, and the remaining signal beam is output conditioned by the detection of the trigger photons [2]. These states must ideally be a particular superposition of odd number of photons, and can constitute superposition states of mesoscopically distinct components, sometimes referred to as the Schrödinger kittens [6, 7].

The negativity of the Wigner function can be easily lost with experimental imperfections. Among them, the imperfections of the homodyne detector are often cor-

rected to reconstruct a Wigner function for a generated state just in front of the homodyne detector. Direct measurement of the negativity of the Wigner function requires a generator with low loss and low noise as well as a nearly ideal homodyne detector. Negative values for the uncorrected Wigner functions were marked, e.g. $W(0, 0) = -0.026$ for the Schrödinger kittens in the photon subtraction scheme [6], and $W(0, 0) = -0.04$ for the single photon state in the non-colinear PDC scheme. (The values correspond to a unit convention according to $\hat{x}\hat{p} - \hat{p}\hat{x} = i$.)

We present a scheme that can generate the photon subtracted squeezed states with the deepest negative dips of the Wigner functions ever observed to our knowledge, including the single photon state and the Schrödinger kittens. Realization of the single photon regime particularly requires a nearly pure squeezed input so as to collect appropriate trigger photons with high signal-to-noise ratio from a small fraction (10% at most) of the squeezed beam, which failed in the previous photon subtraction schemes. Our scheme enables one to vary the regime from the single photon to the Schrödinger kittens by simply tuning the squeezing level which is directly controlled by a pump power for the squeezer, and hence to study continuous transition from the single photon regime to the mesoscopic superposition regime.

II. EXPERIMENT

The key is an optical parametric oscillator (OPO) with a periodically-poled KTiOPO₄ (PPKTP) crystal as a nonlinear medium, which can generate nearly pure squeezed vacuum states in a continuous-wave (cw) regime [8, 9]. A schematic of our experimental setup is shown in Fig.1, which is similar to the previous work [7]. A continuous-wave Ti:Sapphire laser (Coherent MBR110) is used as a primary source of the fundamental beam at 860 nm, which is mainly used to generate second harmonic (430 nm) of about 200 mW by a frequency

*Electronic address: kwakui@nict.go.jp

†Electronic address: psasaki@nict.go.jp

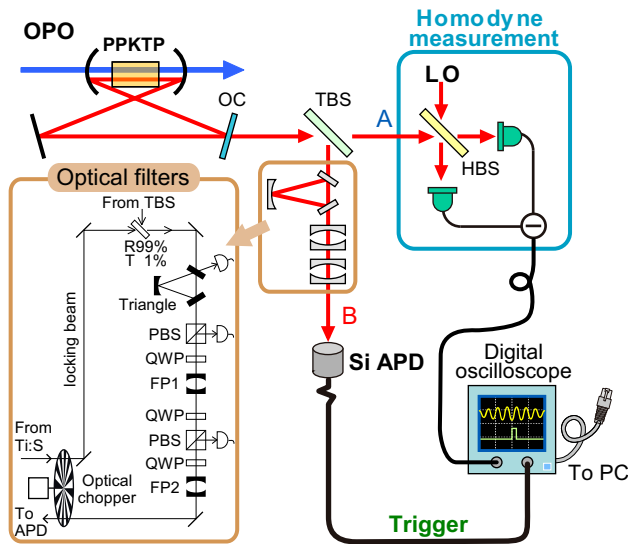


FIG. 1: Schematic of experimental setup. OC:output coupler, TBS:tapping beam splitter, Triangle:triangle cavity, PBS:polarizing beam splitter, QWP:quarter wave plate, FP:Fabry-Perot cavity, HBS:50:50 beam-splitter.

doubler (a bow-tie cavity with KNbO_3), and is also used as a local oscillator (LO) for homodyne detection, and probe beams for various control purposes. The second harmonic beam is used to pump the OPO with a 10 mm long PPKTP crystal (Raicol Crystals) in an optical cavity (a bow-tie configuration with a round-trip length of about 520 mm). An output coupler (OC) of this squeezer cavity has a transmittance of 10.3%, and the intracavity loss is about 0.2~0.3%. The FWHM of the cavity is about 9.3 MHz.

A small fraction (1~10%) of the squeezed vacuum beam in path A is tapped at a beam splitter (TBS), guided into a commercial Si-APD (Perkin Elmer SPCM-AQR-16) through three optical filtering cavities in a row in path B, and is used as trigger signals for conditional photon subtraction. Figure 2 shows a photon counting spectrum of the trigger photons through the filtering cavities, which have 5~10 times wider bandwidths than that of the OPO, measured by detuning the OPO around the fundamental, degenerate, wavelength 860 nm. This consists of a single peak with a bandwidth of 8.6 MHz (FWHM), which can be easily matched with the observable mode by the homodyne detector. Other irrelevant, nondegenerate, modes from the OPO, peaking at every free spectral range of 573 MHz apart from the degenerate frequency, are well suppressed sufficiently. The total transmission ratio for the mode of interest is about 30% just in front of the Si-APD. The trigger counting rate varies from less than 1 kcps up to 50 kcps, changing with the pump power of OPO up to 160 mW and tapping ratios. These trigger counting rates are mostly much greater than the Si-APD dark counts (100 cps).

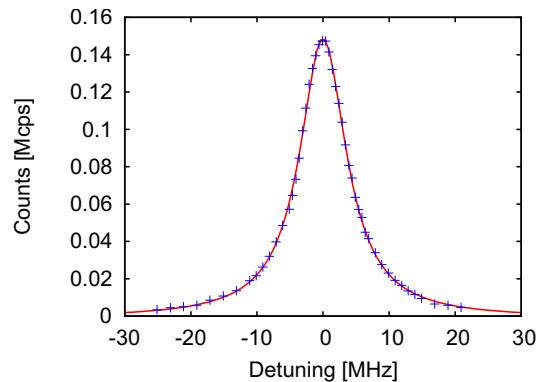


FIG. 2: Photon counting spectrum of the trigger photons through the optical filtering cavities around the degenerate frequency as a function of cavity detuning: solid crosses for experiment, solid line for theory. The pump power was 160 mW. All the OPO output is fed into the APD path for this experiment.

The filter cavities are locked by a “sample-and-hold locking” technique which enables us to switch the system from a “locking phase” to a “measurement phase” periodically. In the locking phase, the filter cavities are locked in a conventional manner (FM-sideband locking technique). On the other hand in the measurement phase, the locking beam is cut off for photon counting and servo amplifiers hold the system in the same state as the one right before the locking beam is cut off. We attain this periodically to have the locking beam of the filters pass one optical chopper two times, before injected into filter cavities and after transmitted them before APD. Shuttered timings are shifted each other in half period with respect to chopping frequency (500 Hz). Uneven duty cycles of chopping disk prevent the locking beam from entering the Si-APD all the time. We also rebuild our servo amplifiers in order to be able to accept external timing signal and switch the two phases synchronized to the optical chopper’s driver.

The generated nonclassical light is combined with the LO at a 50:50 beam-splitter (HBS) and detected by a balanced homodyne detector with Si photodiodes (Hamamatsu S-3759, anti-reflection coated at 860 nm, 99.6% quantum efficiency). In order to improve the homodyne efficiency, the LO beam is spatially filtered by the mode cleaning cavity which yields the same spatial mode as the OPO output. The propagation loss (1~10%) mainly comes from the tapping itself, and the homodyne efficiency is 98%.

For every trigger signal from the Si-APD, a digital oscilloscope (LeCroy WaveRunner 6050A) samples homodyne signals over a period $\sim 0.5 \mu\text{s}$ around the time when the trigger signal is detected, and sends them to a PC one after another. Each segment of the homodyne signals are then time-integrated, being multiplied by a particular temporal mode function $\Psi_0(t)$, to provide

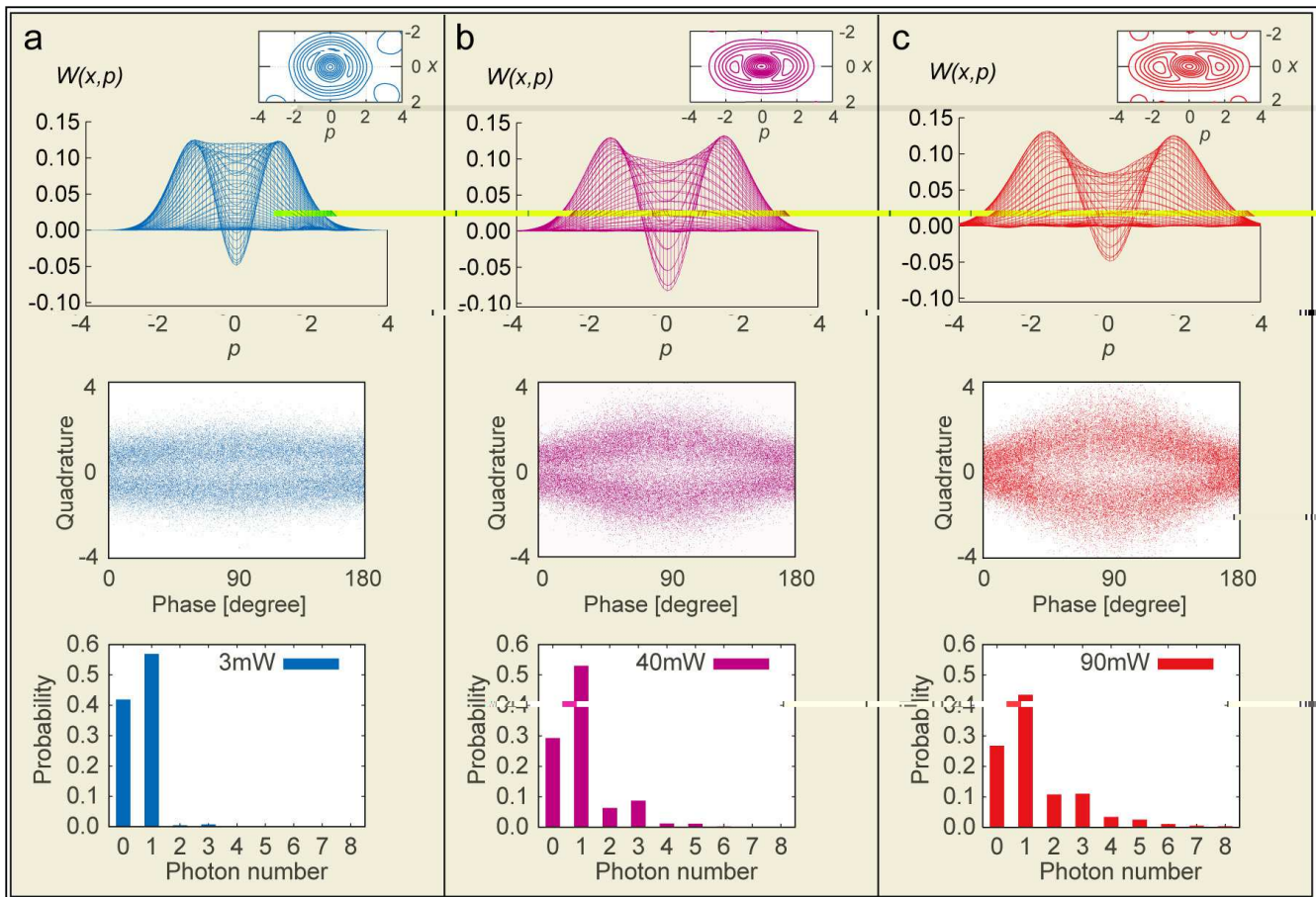


FIG. 3: Experimental Wigner functions (top panels) constructed from raw data without any correction of measurement imperfections in the case of 5% tapping ratio. (a) Single photon state generated by -0.7dB squeezed input. (b) and (c) Schrödinger kittens generated by -2.6dB and -3.7dB squeezed inputs, respectively. The insets in top panels are the contours of the Wigner functions. The middle panels are quadrature distributions obtained by homodyne detection. The bottom panels are photon number distributions obtained by the iterative maximum-likelihood estimation.

the quadrature amplitude finally observed with respect to which the Wigner functions are constructed. About 50,000 data points of the quadrature amplitude are collected, and the Wigner function is constructed using the iterative maximum-likelihood estimation algorithm [10].

III. RESULT AND ANALYSIS

The temporal mode function $\Psi_0(t)$ should be chosen such that it defines the signal mode which shares the maximal entanglement with the trigger photon mode. In the Si-APD, a projection onto photon number states takes place in a time scale $\lesssim 400$ ps. The trigger outputs in this time scale are sent into the digital oscilloscope to sample homodyne signals. The time resolution in this sampling is about $T = 1$ ns. This is slightly longer than the Si-APD time scale, but much shorter than the temporal correlation of the squeezed vacua whose bandwidth is typically $2B \sim 10$ MHz. This T finally defines the trigger photon mode, which can simply be a rectangular tempo-

ral mode function. For such a small BT , a single mode description is valid [11]. In a good approximation, one can consider $\Psi_0(t)$ in a form [12] (see also Appendix A)

$$\Psi_0(t) = \sqrt{\zeta_0} e^{-\zeta_0|t|}, \quad (1)$$

assuming a trigger signal detected at $t = 0$, where $\zeta_0 \equiv (\gamma_T + \gamma_L)/2$ determines the characteristic bandwidth $\zeta_0/\pi \sim 9.3$ MHz of the cavity for the leakage rates $\gamma_T \sim 57$ MHz of the output coupler and $\gamma_L \sim 1.2$ MHz of the cavity loss.

Figure 3 shows experimental Wigner functions (top panels), quadrature distributions over half a period (middle panels), and photon number distributions (bottom panels) of the photon subtracted squeezed states. None of correction of measurement imperfections is made. From the left, the single photon state (Fig. 3a) by -0.7dB squeezed input, and Schrödinger kittens with two kinds of amplitudes (Fig. 3b by -2.6dB squeezed inputs and 3c by -3.7dB squeezed input). The tapping fraction of TBS in Fig. 1 is set to 5%. The large negativity is obtained in a wide range of squeezing levels.

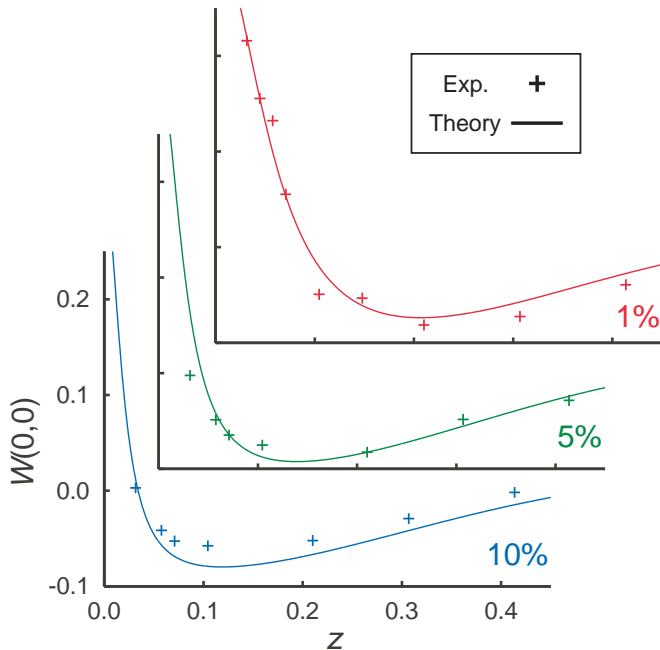


FIG. 4: The dependence of $W(0,0)$ on the squeezing level.

Figure 4 shows the values of the Wigner function at the phase-space origin $W(0,0)$ (solid circles) as a function of the ratio of the pump light amplitude to the threshold amplitude of the OPO, $z = \sqrt{P_{pump}/P_{th}}$, which directly connected to the squeezing level in the cases of three tapping ratios 1%, 5%, and 10%. The lines are fittings by a theoretical model based on the two-mode state reduced to the signal mode $\Psi_0(t)$ and the trigger photon mode $\phi_0(t)$ (Appendix B).

The model includes two kinds of unwanted losses. One is in the homodyne channel modeled by a transmittance $\tau_h = 78\%$, taking imperfections of homodyne electronics into account. The other is a squeezing-level-dependent loss, $\tau_s(z) = \tau_{s0} - \kappa z^2$, which also include a constant linear loss of passive optical elements. The latter is necessary to explain the degradation of the negativity of $W(0,0)$ as z increases. A loss induces a mixing of even-number of states into the photon subtracted squeezed state which ideally contains only odd-number states. Since the values of $W(0,0)$ for even-number of states are positive, the negativity of $W(0,0)$ is easily destroyed by a loss. The z -dependence of $W(0,0)$ cannot be explained by any model with constant linear loss. The optimal fitting is attained for $\tau_{s0} = 0.95$ and $\kappa = 0.93$.

One of main causes for z -dependent loss might be phase fluctuations of the LO in the homodyne detector and of the locking beam at several cavities. Such fluctuations cause effectively phase noises which becomes larger for larger radius in the phase space. As z increases, the Wigner function spreads over the phase space, and suffers from such fluctuations. For realizing larger Schrödinger kittens, it will also be important to suppress phase fluctuations.

tuations.

In the single photon regime, i.e., small z , the trigger count rate becomes small. A primary factor to determine the behavior of $W(0,0)$ is then the noise count rate ν in the trigger channel, which include the dark counts of the Si-APD and background photons. It is necessary to reduce this rate to generate the single photon state with a deep negative Wigner function. In this regard, the OPO with PPKTP works very well to reduce noisy photons.

IV. CONCLUDING REMARKS

We have presented the photon subtracted squeezed states with large negative dips in their Wigner functions. Those highly nonclassical states cover the single photon regime and the Schrödinger kitten regime. Their continuous transition can be controlled by the squeezing level of the input source. The nearly pure input source from the OPO with PPKTP enabled us to study the degradation of the negative Wigner functions in detail. It was found that there was the squeezing-level-dependent loss, whose origins remains open, but we suspect at present that it stems from phase fluctuations of the LO and the locking beam.

Our scheme will particularly be useful to make the output states coupled to atomic media for quantum memory, and also to apply them to spectroscopic applications. In addition, our scheme can directly be combined with well-matured technology of Gaussian operations on quadrature observables in a continuous-wave scheme [13, 14] for pursuing further challenges. For example, the attained level of the nonclassicality, i.e. the large negativity, will allow one to teleport the nonclassicality of non-Gaussian input states, which remains an unreached target in spite of its importance in quantum information science, by using the presently available squeezer with -7dB squeezing [9, 15].

Another important challenge is to combine photon-number resolving detectors [16, 17, 18] with our scheme for breeding the Schrödinger kittens into cats, and for developing a universal quantum gate circuit both for discrete and continuous variables [19, 20, 21].

Acknowledgments

Authors thank K. Hayasaka, J. S. Neergaard-Nielsen, T. Aoki, H. Yonezawa, S. Suzuki and M. Takeoka for their valuable comments and suggestions.

APPENDIX A: MODE FUNCTIONS

To describe the trigger photon mode localized in the time domain, an appropriate basis is given by

$$\phi_k(t) = \begin{cases} \frac{1}{\sqrt{T}} \exp(-i\frac{2\pi kt}{T}) & -\frac{T}{2} \leq t \leq \frac{T}{2}, \\ 0 & \text{otherwise,} \end{cases} \quad (\text{A1})$$

In the present case where $BT \ll 1$, the lowest mode is excited in the Si-APD with the weight $\sim BT$, and the weights of the other higher modes are negligible [11]. The trigger mode function is thus $\phi_0(t)$. The total quantum efficiency for this mode is given by $\eta = \eta_0 \eta_F BT$ where η_0 is the intrinsic quantum efficiency and η_F is the transmittance through the optical filters. Taking a noise count rate ν further into account, detection of the trigger photons is described by the on/off detector POVM as specified in ref. [11].

The signal mode $\Psi_0(t)$ should be appropriately determined by the statistics of the conditional output state $\hat{\rho}_A$ in path A given by

$$\hat{\rho}_A = \frac{\text{Tr}_B[\hat{\rho}_{AB} \hat{\Pi}_{\text{on}}^B(\eta, \nu)]}{\text{Tr}_{AB}[\hat{\rho}_{AB} \hat{\Pi}_{\text{on}}^B(\eta, \nu)]}, \quad (\text{A2})$$

where the state $\hat{\rho}_{AB}$ corresponds to the split beams in paths A and B just after the TBS (Fig. 1). We consider a mode expansion of the field operator to describe the state $\hat{\rho}_A$

$$\hat{A}(t) \sim \sum_{k=0}^{K-1} \hat{A}_k \Psi_k(t), \quad (\text{A3})$$

where

$$\int_{-\infty}^{\infty} dt \Psi_k^*(t) \Psi_k(t) = \delta_{kl}. \quad (\text{A4})$$

The mode functions $\{\Psi_k(t)\}$ are determined by minimizing the square error

$$\begin{aligned} J_K &= \text{Tr} \left[\int_{-\infty}^{\infty} dt \left| \hat{A}(t) - \sum_{k=0}^{K-1} \hat{A}_k \Psi_k(t) \right|^2 \right] \\ &= \int_{-\infty}^{\infty} dt \text{Tr} [\hat{A}^\dagger(t) \hat{A}(t)] - \sum_{k=0}^{K-1} \text{Tr} [\hat{A}_k^\dagger \hat{A}_k]. \end{aligned} \quad (\text{A5})$$

Since the first term is constant, we are to maximize the second term under the constraint of Eq. (A4) for each k . It is known that the optimal solution for this is given by the eigenfunctions of the integral equation

$$\chi_k \Psi_k(t) = \int_{-\infty}^{\infty} dt' h(t, t') \Psi_k(t'), \quad (\text{A6})$$

where

$$h(t, t') = \text{Tr}_A[\hat{\rho}_A \hat{A}^\dagger(t) \hat{A}(t')], \quad (\text{A7})$$

assuming that the trigger signal is detected at $t = 0$ [11, 12].

In a good approximation, one can consider only the lowest order mode $\Psi_0(t)$ in a form

$$\Psi_0(t) = \sqrt{\zeta_0} e^{-\zeta_0 |t|}. \quad (\text{A8})$$

The Wigner function is constructed with respect to the field component defined by

$$\hat{A} \equiv \hat{A}_0 = \int_{-\infty}^{\infty} dt \hat{A}(t) \Psi_0(t). \quad (\text{A9})$$

APPENDIX B: FORMULA OF WIGNER FUNCTION

The Wigner function can be obtained by evaluating the covariance matrices in terms of the signal mode $\Psi_0(t)$ and the trigger photon mode $\phi_0(t)$ as prescribed in ref. [12], exploiting the on/off detector model in ref. [11]:

$$W(x, p) = \frac{R(x, p; 0, 0) - R(x, p; \eta, \nu)}{1 - \mathcal{N}(\eta, \nu)}, \quad (\text{B1})$$

where

$$\begin{aligned} R(x, p; \eta, \nu) &= \frac{\mathcal{N}(\eta, \nu)}{\pi \sqrt{[1 - \tau_h + \tau_h \sigma^2(z)] [1 - \tau_h + \tau_h \sigma^2(-z)]}} \\ &\times \exp\left(-\frac{x^2}{1 - \tau_h + \tau_h \sigma^2(z)} - \frac{p^2}{1 - \tau_h + \tau_h \sigma^2(-z)}\right), \end{aligned} \quad (\text{B2})$$

with

$$\mathcal{N}(\eta, \nu) = \frac{2e^{-\nu}}{\sqrt{\{2 + [b(z) - 1] \eta\} \{2 + [b(-z) - 1] \eta\}}}, \quad (\text{B3})$$

and

$$\sigma^2(z) = a(z) - \frac{c^2(z) \eta}{2 + [b(z) - 1] \eta}, \quad (\text{B4})$$

where

$$a(z) = 1 - \tau + \tau \left[1 - \frac{2\tau_s(z) \gamma_T}{\zeta_0} \frac{z(z+3)}{(z+1)(z+2)^2} \right], \quad (\text{B5})$$

$$b(z) = \tau + (1 - \tau) \left(1 - \tau_s(z) \gamma_T T \frac{z}{z+1} \right), \quad (\text{B6})$$

$$c(z) = \sqrt{(1 - \tau) \tau} \frac{2\tau_s(z) \gamma_T \sqrt{T}}{\sqrt{\zeta_0}} \frac{z}{(z+1)(z+2)}, \quad (\text{B7})$$

Here τ is the transmittance of TBS in Fig. 1, τ_h is the effective transmittance of the homodyne channel, and $\tau_s(z) = \tau_{s0} - \kappa z^2$ is a phenomenological model for a squeezing-level-dependent loss, which is necessary to explain the degradation of the negativity of $W(0, 0)$ as z increases.

-
- [1] B. Yurke and D. Stoler, Phys. Rev. A **36**, 1955 (1987).
- [2] M. Dakna, T. Anhut, T. Opatrný, L. Knöll, and D.-G. Welsch, Phys. Rev. A **55**, 3184 (1997).
- [3] A. I. Lvovsky, et al., Phys. Rev. Lett. **87**, 050402 (2001); A. Zavatta, S. Viciani, and M. Bellini, Phys. Rev. A **70**, 053821 (2004).
- [4] A. Ourjoumtsev, et. al., quant-ph0608230.
- [5] A. I. Lvovsky, and S. A. Babichev, Phys. Rev. A **66**, 011801 (2002); A. Zavatta, S. Viciani, and M. Bellini, Science **306**, 660-662 (2004).
- [6] A. Ourjoumtsev, et al., Science **312**, 83 (2006).
- [7] J. S. Neergaard-Nielsen, et.al., Phys. Rev. Lett.**97**, 083604 (2006).
- [8] T. Aoki et al., Opt. Exp. **14**, 6930 (2006).
- [9] S. Suzuki et al., Appl. Phys. Lett., **89**, 061116 (2006).
- [10] A. I. Lvovsky, J. Opt. B: Quantum Semiclass. Opt. **6**, S556 (2004).
- [11] M. Sasaki, and S. Suzuki, Phys. Rev. A **73**, 043807 (2006).
- [12] K. Mølmer, Phys. Rev. A **73**, 063804 (2006).
- [13] H. Yonezawa et al., Nature **431**, 430 (2004).
- [14] N. Takei et al., Phys. Rev. Lett.**94**, 220502 (2005).
- [15] S. L. Braunstein and H. J. Kimble, Phys. Rev. Lett.**80**, 869 (1998).
- [16] E. Waks, et al., Phys. Rev. Lett. **92**, 113602 (2004)
- [17] D. Rosenberg, et al., Phys. Rev. A **71**, 061803, (2005).
- [18] M. Fujiwara, and M. Sasaki, Opt. Lett., **31**, 691 (2006).
- [19] D. Gottesman, A. Kitaev, and J. Preskill, Phys. Rev. A**64**, 012310 (2001).
- [20] S. D. Bartlett and B. C. Sanders, Phys. Rev. A**65**, 042304 (2002).
- [21] M. Sasaki, et al., *Quantum Communication, Measurement and Computing*, 44, (eds. S. M. Barnett et al., AIP, New York, 2004); quant-ph/0601058.